Contribution from the Department of Chemistry,
University of Missouri—Columbia, Columbia, Missouri 65211

Synthesis and Characterization of a Platinum–Mercury "A-Frame" Cluster

Paul R. Sharp

Received April 7, 1986

The reaction of $Pt_2Cl_2(dppm)_2$ (dppm = bis(diphenylphosphino)methane) with $HgCl_2$ gives orange, crystalline $Pt_2(\mu\text{-}HgCl_2)Cl_2(dppm)_2$. The complex was characterized by solution NMR and a crystal structure determination. The crystals are triclinic ($P\bar{1}$) with $a = 11.5873$ (3) Å, $b = 22.1559$ (5) Å, $c = 23.0359$ (5) Å, $\alpha = 65.53$ (2)°, $\beta = 76.53$ (2)°, $\gamma = 84.30$ (2)°, $V = 5234.7$ Å^3, and $Z = 4$. The three-dimensional X-ray data were measured by the θ–2θ scan technique with a scintillation detector. The structure was resolved by direct and Fourier methods and refined by full-matrix least-squares calculations to give $R = 0.032$ and $R_w = 0.041$ for 5773 observations above 2σ. The solid-state structure consists of two nearly identical, independent, triangular clusters and two independent, half-occupancy CH_2Cl_2 molecules of crystallization. Each cluster has an "A-frame" structure with $HgCl_2$ at the apex bridging the two bonded Pt atoms. The geometry about the Hg atom is that of a flattened tetrahedron.

Introduction

Molecular "A-frame"[1] complexes (**1**) are a well-developed class of bimetallic complexes. Examples are known with a large variety of small molecules/fragments bridging in the apex position X.[1,2] The possibility of extending the "A-frame" class to include trimetallic clusters (X = a metal fragment) was suggested several years ago in a theoretical study by Hoffman and Hoffmann on "A-frame" complexes.[3] On the basis of the isolobal relationship between the methylene group and the ML_2 d^{10} and ML_4 d^8 transition-metal fragments[4] (see Figure 1) "A-frame" clusters derived from known "A-frame" complexes by replacing a methylene group with an ML_2 or ML_4 fragment (X = ML_2 or ML_4) were predicted to be stable. While several clusters have been prepared from "A-frame" precursors (e.g. $Pt_2Cl_2(dppm)_2$), none of these have an "A-frame" structure.[5] Recently, the isolation of a Rh cluster that can be viewed as a derivative of the predicted type was reported.[6] The absence of any simple examples of the predicted "A-frame" clusters was attributed to the inability of generating, under mild conditions, the unsaturated metal fragments needed to react with the "A-frame" precursors.

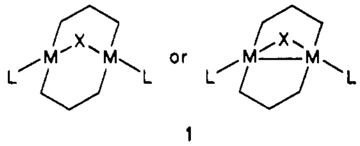

1

While working on the preparations of oxygen atom bridged "A-frame" complexes (X = O),[7] we found that $HgCl_2$, formally an ML_2 d^{10} fragment, readily forms a trimetallic "A-frame" cluster with $HgCl_2$ at the apex. The NMR and structural data indicate that the bonding in this cluster is different from that predicted for the clusters considered by Hoffman and Hoffmann. Instead, the $HgCl_2$ bonding in the cluster appears to be predominantly of a_1 symmetry with little or no b_2 contribution. This result is not unexpected, considering the requirement for ML_2 d-orbital participation in the b_2 interaction and the low energy of the Hg d orbitals.

Table I. ^{31}P NMR Data for $[Pt_2(\mu\text{-}Y)X_2(dppm)_2]^z$

Y, X, z	δ	$^1J_{PtP}$, Hz	$^2J_{PtP}$, Hz	$^2J_{PP}$, Hz	$^3J_{PP}$, Hz	ref
$HgCl_2$, Cl, 0	10.2	2295	−64	58	24	*a*
H, Cl, +1	6.6	2317	−40	52	21	9
H, Me, +1	13.5	2884	24	51	15	12
H, H, +1	17.9	2770	16	56	18	10
Cl, H, +1	12.9	2605	0	55	17	10
–, Cl, 0	0.0	2936	−136	62	26	8
CH_2, Cl, 0	10.0	3388	73	23	6	20
SO_2, Cl, 0	19.5	3588	273	43	0	20

[a] This work; solvent $CDCl_3$; $^2J_{PHg} = 151.2$ Hz.

Results and Discussion

A yellow solution of $Pt_2Cl_2(dppm)_2$ (**2**) in methylene chloride rapidly turns orange when 1 equiv of $HgCl_2$ is added. From this

$$\underset{\mathbf{2}}{Pt_2Cl_2(dppm)_2} + HgCl_2 \rightarrow \underset{\mathbf{3}}{Pt_2(\mu\text{-}HgCl_2)Cl_2(dppm)_2} \qquad (1)$$

solution orange crystals can be isolated in high yield by the addition of diethyl ether. NMR spectral data, discussed below, indicate the incorporation of Hg into the complex and the probable formation of the "A-frame" complex **3**. This was confirmed by an X-ray crystal structure determination.

NMR Spectra. As a result of the 33.8% natural abundance of a Pt isotope with a spin of $^1/_2$ (^{195}Pt) the ^1H and ^{31}P NMR spectra of binuclear Pt complexes typically consist of superimposed spectra for three different isotopomers: one with no ^{195}Pt atoms (43.8%), one with one ^{195}Pt atom (44.8%), and one with two ^{195}Pt atoms (11.4%). NMR data are therefore extremely useful for analyzing the structure and bonding.[8] ^{31}P NMR data for **3** and related binuclear Pt complexes are listed in Table I.

The ^{31}P NMR spectrum of **3** is similar to that of **2** and other dppm-bridged Pt dimers, showing the expected pattern for the three different isotopomers. The assorted coupling constants are considered to be diagnostic of the bonding in complexes based on the $Pt_2(dppm)_2$ core.[9] The coupling constants for **3** closely resemble those for $[Pt_2(\mu\text{-}H)Cl_2(dppm)_2]^+$ (obtained by protonation of $Pt_2Cl_2(dppm)_2$),[10] suggesting similar bonding in these two complexes: that is, the bondings of H^+ and $HgCl_2$ to the $Pt_2Cl_2(dppm)_2$ fragment are similar. Since the interaction of H^+ is only of a_1 symmetry, this must also be true of $HgCl_2$. Other indications of this are found in the structural parameters discussed below.

An additional feature in the ^{31}P NMR spectrum of **3**, not present in the spectra of the other bimetallic Pt complexes, are

---

(1) Kubiak, C. P.; Eisenberg, R. *J. Am. Chem. Soc.* **1977**, *99*, 6129–6131; *Inorg. Chem.* **1980**, *19*, 2726–2732.

(2) Puddephatt, R. J. *Chem. Soc. Rev.* **1983**, *12*, 99–128. Jandik, P.; Schubert, U.; Schmidbaur, H. *Angew. Chem., Int. Ed. Engl.* **1982**, *21*, 72. *Angew. Chem. Suppl.* **1982**, 1–12. Murray, H. H.; Fackler, J. P., Jr.; Mazany, A. M. *Organometallics* **1984**, *3*, 1310–1311. Knachel, H. C.; Dudis, D. S.; Fackler, J. P., Jr. *Ibid.* **1984**, *3*, 1312–1313. Murray, H. H.; Mazany, A. M.; Fackler, J. P., Jr. *Ibid.* **1985**, *4*, 154–157.

(3) Hoffman, D. M.; Hoffmann, R. *Inorg. Chem.* **1981**, *20*, 3543–3555.

(4) Mingos, D. M. P. *J. Chem. Soc., Dalton Trans.* **1977**, 602–610; *Adv. Organomet. Chem.* **1977**, *15*, 1. Hoffmann, P. *Angew. Chem., Int. Ed. Engl.* **1977**, *16*, 536–537. Elian, M.; Mingos, D. M. P.; Hoffmann, R. *Inorg. Chem.* **1975**, *14*, 1058–1076. Burdett, J. K. *J. Chem. Soc., Faraday Trans. 2* **1974**, *70*, 1599–1613.

(5) Braunstein, P.; Kervennal, J.; Richert, J.-L. *Angew. Chem., Int. Ed. Engl.* **1985**, *24*, 768–770. Braunstein, P.; de Meric de Bellefon, C.; Ries, M. *J. Organomet. Chem.* **1984**, *262*, C14–C18. Grossel, M. C.; Moulding, R. P.; Seddon, K. R. *J. Organomet. Chem.* **1983**, *253*, C50–C54. Braunstein, P.; Jud, J.-M.; Dusausoy, Y.; Fischer, J. *Organometallics* **1983**, *2*, 180–183.

(6) Deraniyagala, S. P.; Grundy, K. R. *J. Chem. Soc., Dalton Trans.* **1985**, 1577–1583.

(7) Paper presented at the 190th National Meeting of the American Chemical Society, Chicago, 1985. Manuscript in preparation.

(8) Brown, M. P.; Puddephatt, R. J.; Rashidi, M.; Seddon, K. R. *J. Chem. Soc., Dalton Trans.* **1977**, 951–955.

(9) Brown, M. P.; Fisher, J. R.; Franklin, S. J.; Puddephatt, R. J.; Seddon, K. R. *J. Organomet. Chem.* **1978**, *161*, C46–C48.

(10) Brown, M. P.; Puddephatt, R. J.; Rashidi, M.; Seddon, K. R. *J. Chem. Soc., Dalton Trans.* **1978**, 516–522.

0020-1669/86/1325-4185$01.50/0

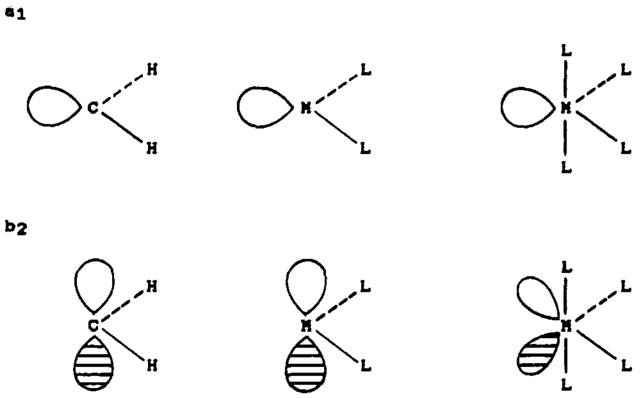

Figure 1. Frontier orbitals of CH_2, ML_2 d^{10}, and ML_4 d^8.

satellites centered around the central peak (isotopomer with no ^{195}Pt). These can be attributed to ^{31}P coupling to the ^{199}Hg (17% abundance) of the $HgCl_2$ group. (Presumably, the other isotopomers display similar satellites, but these are too weak to observe.)

The ^1H NMR spectrum of **3** shows the distinct AB pattern for the dppm methylenes typical of "A-frame" complexes. This AB pattern arises from the positioning of the methylene protons on either the same or the opposite side of the bridging apex group. In addition to the AB coupling, coupling to ^{31}P and ^{195}Pt can be observed. Often, one of the methylene protons shows a much larger coupling to ^{195}Pt, which ranges from 30 to 80 Hz. While this is true in the present case, the ^{195}Pt coupling is unusually large at 97.8 Hz. The other methylene proton coupling to ^{195}Pt is typical at 11.4 Hz. We suspect the large coupling is a result of steric interactions between the methylene groups and the chlorides of the $HgCl_2$ group (see below).

Stability of $Pt_2(\mu\text{-}HgCl_2)Cl_2(dppm)_2$. The reaction in eq 1 is analogous to the protonation of $Pt_2Cl_2(dppm)_2$ (eq 2).[10] The

$$Pt_2Cl_2(dppm)_2 + H^+ \rightleftharpoons [Pt_2(\mu\text{-}H)Cl_2(dppm)_2]^+ \qquad (2)$$

protonation reaction is reversible,[10,11] and we were interested to see if this was true of the $HgCl_2$ reaction. To test this possibility, an equimolar mixture of **2** and **3** was dissolved in chlorobenzene and ^{31}P NMR spectra were recorded at 100 °C. If the reaction were reversible, exchange of the two signals should be observed (eq 3). No indication of exchange was detected; all lines remained

$$Pt_2Cl_2(dppm)_2 + Pt_2(\mu\text{-}HgCl_2)Cl_2(dppm)_2 \rightleftharpoons Pt_2(\mu\text{-}HgCl_2)Cl_2(dppm)_2 + Pt_2Cl_2(dppm)_2 \qquad (3)$$

sharp. The irreversibility of the reaction was also evident by the retention of ^{31}P coupling to ^{199}Hg in the signal for **3**.

Thermally, the cluster is quite robust. The chlorobenzene from the above NMR sample was boiled off in air with no detectable decomposition. The solid is stable to 290 °C, above which temperature the color fades irreversibly from orange to white.

Solid-State Structure of $Pt_2(\mu\text{-}HgCl_2)Cl_2(dppm)_2$. Crystal data and experimental parameters are given in Table II. Two nearly identical independent molecules of $Pt_2(\mu\text{-}HgCl_2)Cl_2(dppm)_2$ are present in the asymmetric unit with no crystallographically imposed symmetry. A perspective view of molecule A is shown in Figure 2. A similar view of molecule B is provided as supplementary material (Figure S1). Refined atom fractional coordinates are given in Table III, and selected intramolecular distances and angles are given in Tables IV–VI. The differences between molecule A and molecule B are slight, and in the following discussion data for molecule A will be given with data for molecule B in parentheses.

Table II. Crystallographic and Data Collection Parameters[a]

space group	$P\bar{1}$
formula	$Pt_2HgCl_5P_4C_{50.5}H_{45}$[b]
a, Å	11.587 (3)
b, Å	22.156 (5)
c, Å	23.036 (5)
α, deg	65.53 (2)
β, deg	76.53 (2)
γ, deg	84.30 (2)
V, Å^3	5234.7
ρ(calcd) (ρ(measd)), g cm^{-3}	1.96[b] (2.01)
Z	4
no. of reflecns measd	9394
unique data	8393
data above 2σ	5773
no. of params refined	738
R	0.032
R_w	0.041
gof	1.688
diffractometer	Enraf-Nonius CAD-4
cryst size, mm	0.3 × 0.2 × 0.07
λ, Å (Mo Kα)	0.71073
μ, cm^{-1}	71.6
abs cor method	empirical (ψ scan)
transmission range, %	32.8–99.9
scan time	variable to maintain 3% counting stats (90 s max)
θ–2θ scan	96 steps/scan
bkgd	16 steps on each side of peak
peak	64 steps
takeoff angle, deg	2.8
scan width, θ	0.65 + 0.35 tan θ
$2\theta_{max}$, deg	38
khl range	±*h*,±*k*,+*l*

[a] Here and in the following tables the numbers in parentheses represent the error in the least significant digit(s). [b] Assuming 0.5 molecules of CH_2Cl_2 per formula unit.

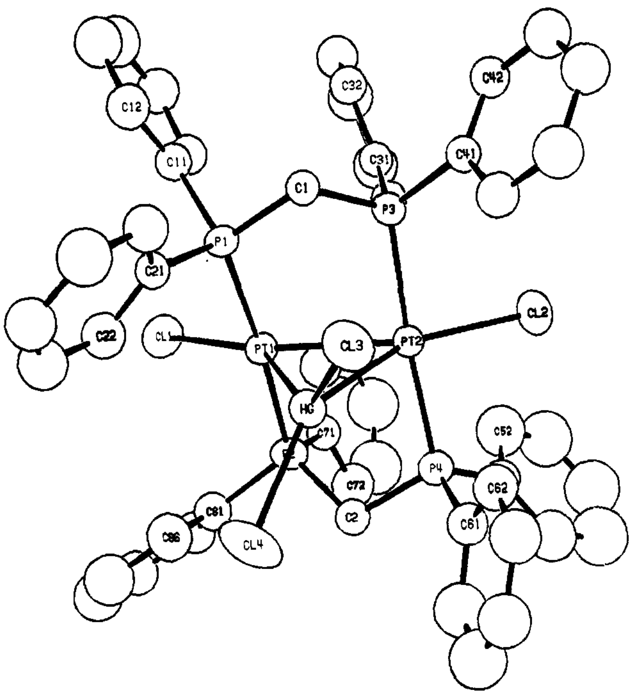

Figure 2. ORTEP drawing of $Pt_2(\mu\text{-}HgCl_2)Cl_2(dppm)_2$, molecule A, with 50% probability ellipsoids and spheres (phenyl ring carbons). Phenyl ring carbon atoms are numbered consecutively around the ring.

The overall structure is typical of the "A-frame" class. The pseudo-six-membered ring formed by the Pt atoms and the dppm ligands is in the more common boat configuration with the methylene carbon atoms tipped toward the apex. (A framework molecular model suggests that this orientation gives the most flexible structure.) The chlorides have bent away from the apexial $HgCl_2$ group, and the Pt, Cl, and Hg atom are, as expected, all coplanar (largest devition is 0.028 Å (0.029 Å)). However, other features differ significantly from those of a typical "A-frame" complex.

---

(11) Puddephatt, R. J.; Azam, K. A.; Hill, R. H.; Brown, M. P.; Nelson, C. D.; Moulding, R. P.; Seddon, K. R.; Grossel, M. C. *J. Am. Chem. Soc.* **1983**, *105*, 5642–5646.

Table III. Positional Parameters for Refined Atoms[a]

atom	*x*	*y*	*z*	*B*, Å^2	atom	*x*	*y*	*z*	*B*, Å^2
Molecule A									
Hg	0.62236 (5)	0.22423 (3)	0.78321 (3)	3.07 (2)	C41	0.820 (1)	0.0795 (7)	0.9606 (7)	3.1 (4)*
Pt1	0.82441 (5)	0.29418 (3)	0.74913 (3)	2.57 (2)	C42	0.884 (1)	0.0532 (8)	1.0087 (8)	3.6 (4)*
Pt2	0.83416 (5)	0.16026 (3)	0.79159 (3)	2.72 (2)	C43	0.847 (1)	−0.0043 (9)	1.0607 (8)	4.5 (4)*
Cl1	0.8962 (4)	0.4023 (2)	0.7069 (2)	5.0 (1)	C44	0.750 (2)	−0.0388 (9)	1.0670 (8)	4.7 (4)*
Cl2	0.9118 (5)	0.0531 (2)	0.8230 (2)	6.4 (2)	C45	0.685 (2)	−0.0141 (9)	1.0180 (9)	5.3 (5)*
Cl3	0.4958 (4)	0.1561 (2)	0.8868 (2)	4.5 (1)	C46	0.722 (1)	0.0448 (8)	0.9640 (8)	4.4 (4)*
Cl4	0.4930 (4)	0.2722 (3)	0.7067 (3)	6.1 (2)	C51	0.939 (2)	0.1147 (7)	0.6600 (7)	4.2 (5)
P1	0.7591 (4)	0.2950 (2)	0.8515 (2)	2.6 (1)	C52	1.052 (2)	0.121 (1)	0.662 (1)	7.4 (7)
P2	0.8750 (4)	0.3009 (2)	0.6438 (2)	3.1 (1)	C53	1.140 (2)	0.089 (1)	0.639 (1)	9.1 (8)
P3	0.8527 (4)	0.1570 (2)	0.8899 (2)	2.8 (1)	C54	1.122 (2)	0.050 (1)	0.611 (1)	10.9 (8)
P4	0.8158 (4)	0.1558 (2)	0.6965 (2)	3.5 (1)	C55	1.013 (2)	0.041 (1)	0.610 (1)	11.5 (8)
C1	0.748 (1)	0.2107 (7)	0.9169 (7)	2.4 (3)*	C56	0.917 (2)	0.0734 (9)	0.633 (1)	6.9 (7)
C2	0.806 (1)	0.2398 (7)	0.6329 (7)	3.0 (4)*	C61	0.678 (1)	0.1159 (8)	0.7089 (8)	4.3 (4)*
C11	0.842 (1)	0.3394 (7)	0.8786 (7)	2.8 (4)*	C62	0.619 (1)	0.0767 (8)	0.7713 (8)	4.4 (4)*
C12	0.784 (2)	0.3564 (9)	0.9280 (9)	4.9 (5)*	C63	0.507 (2)	0.053 (1)	0.780 (1)	6.1 (5)*
C13	0.849 (2)	0.386 (1)	0.9558 (9)	6.1 (5)*	C64	0.455 (2)	0.070 (1)	0.7277 (9)	5.9 (5)*
C14	0.964 (2)	0.396 (1)	0.931 (1)	6.9 (6)*	C65	0.513 (2)	0.105 (1)	0.664 (1)	7.3 (6)*
C15	1.022 (2)	0.3799 (9)	0.8817 (9)	4.8 (5)*	C66	0.625 (2)	0.129 (1)	0.655 (1)	6.8 (6)*
C16	0.959 (1)	0.3497 (8)	0.8534 (8)	4.1 (4)*	C71	1.030 (1)	0.2926 (8)	0.6151 (6)	3.5 (5)
C21	0.609 (1)	0.3290 (8)	0.8589 (7)	3.2 (4)*	C72	1.071 (2)	0.283 (1)	0.5595 (9)	6.2 (7)
C22	0.583 (1)	0.3791 (9)	0.8034 (8)	4.6 (4)*	C73	1.192 (2)	0.279 (1)	0.538 (1)	9.6 (9)
C23	0.469 (2)	0.4078 (9)	0.8074 (9)	5.5 (5)*	C74	1.269 (2)	0.280 (1)	0.572 (1)	10.9 (9)
C24	0.389 (2)	0.3852 (9)	0.8663 (9)	5.1 (5)*	C75	1.230 (2)	0.288 (1)	0.627 (1)	8.4 (8)
C25	0.415 (2)	0.3353 (9)	0.9198 (9)	5.7 (5)*	C76	1.109 (2)	0.296 (1)	0.6490 (9)	5.9 (7)
C26	0.527 (1)	0.3061 (8)	0.9172 (8)	4.2 (4)*	C81	0.827 (1)	0.3771 (8)	0.5873 (8)	4.0 (5)
C31	0.997 (1)	0.1820 (7)	0.8856 (7)	2.8 (4)*	C82	0.901 (2)	0.4182 (9)	0.5300 (9)	5.3 (5)*
C32	1.024 (1)	0.1988 (8)	0.9332 (8)	3.7 (4)*	C83	0.858 (2)	0.479 (1)	0.4878 (9)	5.9 (5)*
C33	1.137 (2)	0.2223 (9)	0.9247 (9)	4.9 (5)*	C84	0.748 (2)	0.497 (1)	0.500 (1)	7.4 (6)*
C34	1.220 (2)	0.2295 (9)	0.8702 (9)	4.8 (5)*	C85	0.670 (2)	0.458 (1)	0.556 (1)	6.7 (6)*
C35	1.196 (2)	0.2149 (9)	0.8232 (9)	5.7 (5)*	C86	0.710 (2)	0.3968 (9)	0.5990 (9)	5.4 (5)*
C36	1.086 (1)	0.1916 (8)	0.8292 (8)	4.0 (4)*					
CH_2Cl_2 Solvate of Molecule A									
ClS1	0.8177 (9)	0.4863 (6)	0.2644 (6)	8.3 (4)	CS	0.803 (4)	0.532 (2)	0.296 (2)	8 (1)*
ClS2	0.707 (1)	0.5734 (6)	0.3154 (6)	13.8 (4)					
Molecule B									
Hg	0.69902 (6)	0.23504 (4)	0.27152 (3)	3.86 (2)	C41	0.610 (1)	0.4449 (8)	0.1181 (7)	3.2 (4)*
Pt1	0.46220 (6)	0.22376 (3)	0.31804 (3)	2.70 (2)	C42	0.569 (1)	0.4960 (8)	0.0670 (8)	4.0 (4)*
Pt2	0.55208 (5)	0.27729 (3)	0.18636 (3)	2.50 (2)	C43	0.649 (2)	0.5387 (9)	0.0156 (9)	5.3 (5)*
Cl1	0.3289 (5)	0.1815 (2)	0.4186 (2)	5.4 (2)	C44	0.769 (2)	0.5320 (9)	0.0147 (9)	5.2 (5)*
Cl2	0.5587 (4)	0.3285 (2)	0.0736 (2)	4.0 (1)	C45	0.812 (2)	0.4837 (9)	0.0645 (9)	4.9 (5)*
Cl3	0.8559 (4)	0.3129 (3)	0.2484 (3)	8.5 (2)	C46	0.733 (1)	0.4406 (8)	0.1153 (8)	4.4 (4)*
Cl4	0.7855 (4)	0.1264 (3)	0.3268 (3)	6.0 (2)	C51	0.508 (1)	0.1664 (7)	0.1245 (7)	2.6 (3)*
P1	0.4666 (4)	0.3213 (2)	0.3307 (2)	3.6 (1)	C52	0.399 (1)	0.1955 (8)	0.1182 (7)	3.3 (4)*
P2	0.4381 (4)	0.1251 (2)	0.3106 (2)	2.8 (1)	C53	0.332 (2)	0.1817 (9)	0.0829 (8)	4.8 (5)*
P3	0.5159 (4)	0.3817 (2)	0.1846 (2)	2.9 (1)	C54	0.373 (2)	0.1415 (9)	0.0530 (9)	4.8 (5)*
P4	0.5921 (4)	0.1782 (2)	0.1766 (2)	2.8 (1)	C55	0.478 (2)	0.1133 (9)	0.0570 (9)	5.2 (5)*
C1	0.540 (1)	0.3886 (8)	0.2559 (8)	4.2 (4)*	C56	0.550 (1)	0.1232 (8)	0.0923 (8)	4.3 (4)*
C2	0.558 (1)	0.1073 (7)	0.2545 (7)	2.9 (4)*	C61	0.747 (1)	0.1670 (7)	0.1469 (7)	3.0 (4)*
C11	0.321 (1)	0.3555 (8)	0.3482 (8)	3.7 (4)*	C62	0.817 (1)	0.2206 (9)	0.1076 (8)	4.6 (4)*
C12	0.303 (2)	0.409 (1)	0.370 (1)	6.7 (6)*	C63	0.940 (2)	0.213 (1)	0.0858 (9)	5.8 (5)*
C13	0.190 (2)	0.434 (1)	0.381 (1)	6.8 (6)*	C64	0.987 (2)	0.1492 (9)	0.1025 (9)	4.9 (5)*
C14	0.101 (2)	0.412 (1)	0.374 (1)	7.3 (6)*	C65	0.918 (1)	0.0992 (9)	0.1417 (8)	4.6 (4)*
C15	0.113 (2)	0.362 (1)	0.352 (1)	6.3 (5)*	C66	0.798 (1)	0.1063 (8)	0.1621 (8)	4.2 (4)*
C16	0.223 (1)	0.3338 (8)	0.3418 (8)	4.2 (4)*	C71	0.303 (1)	0.1281 (7)	0.2822 (7)	3.2 (4)*
C21	0.539 (2)	0.3199 (8)	0.3896 (7)	4.3 (5)	C72	0.277 (1)	0.0778 (8)	0.2668 (8)	3.6 (4)*
C22	0.527 (2)	0.271 (1)	0.444 (1)	9.6 (8)	C73	0.174 (2)	0.0796 (9)	0.2458 (9)	5.0 (5)*
C23	0.577 (3)	0.267 (1)	0.497 (1)	11 (1)	C74	0.098 (2)	0.1269 (9)	0.2421 (9)	5.4 (5)*
C24	0.629 (2)	0.323 (1)	0.4889 (9)	9.3 (8)	C75	0.123 (2)	0.1803 (9)	0.2553 (8)	4.8 (5)*
C25	0.642 (3)	0.370 (1)	0.434 (1)	15 (1)	C76	0.227 (1)	0.1801 (8)	0.2756 (8)	3.6 (4)*
C26	0.600 (2)	0.366 (1)	0.387 (1)	17.8 (9)	C81	0.427 (1)	0.0478 (7)	0.3839 (7)	2.9 (4)*
C31	0.365 (1)	0.4054 (7)	0.1804 (7)	3.1 (4)*	C82	0.316 (1)	0.0243 (8)	0.4201 (8)	4.1 (4)*
C32	0.316 (1)	0.4645 (9)	0.1888 (8)	4.4 (4)*	C83	0.310 (2)	−0.035 (1)	0.4770 (9)	6.0 (5)*
C33	0.199 (2)	0.4771 (9)	0.1899 (9)	5.6 (5)*	C84	0.407 (1)	−0.0687 (9)	0.4921 (8)	4.7 (5)*
C34	0.127 (2)	0.4365 (9)	0.1813 (9)	5.4 (5)*	C85	0.517 (1)	−0.0466 (8)	0.4560 (8)	4.5 (4)*
C35	0.171 (2)	0.3824 (9)	0.1732 (9)	4.8 (5)*	C86	0.525 (1)	0.0130 (8)	0.4012 (8)	3.7 (4)*
C36	0.292 (1)	0.3665 (8)	0.1740 (8)	3.6 (4)*					
CH_2Cl_2 Solvate of Molecule B									
CS	0.982 (4)	0.177 (2)	0.423 (2)	9 (1)*	ClS2	0.880 (1)	0.2131 (7)	0.4610 (7)	10.8 (5)
ClS1	1.012 (1)	0.1051 (7)	0.4401 (6)	8.4 (4)					

[a] Values marked with an asterisk are for atoms refined isotropically. Thermal parameters for atoms C71 of molecule A and C26 of molecule B are non positive definite.

Table IV. Selected Intramolecular Distances (Å)

atom		molecule	
1	2	A	B
Hg	Pt1	2.7122 (8)	2.6991 (8)
Hg	Pt2	2.7153 (7)	2.7097 (8)
Hg	Cl3	2.440 (4)	2.445 (4)
Hg	Cl4	2.417 (4)	2.448 (5)
Pt1	Pt2	2.7119 (8)	2.7361 (9)
Pt1	Cl1	2.338 (4)	2.336 (4)
Pt1	P1	2.310 (4)	2.304 (4)
Pt1	P2	2.305 (4)	2.311 (4)
Pt2	Cl2	2.330 (4)	2.350 (4)
Pt2	P3	2.297 (4)	2.295 (4)
Pt2	P4	2.291 (4)	2.291 (4)
P1	P3	2.975 (5)	2.995 (5)
P2	P4	3.016 (6)	2.990 (5)

A slight twist of the two P–M–P vectors is often observed in "A-frame" structures. In **3** this twist is unusually large as reflected in the torsional angles P1–Pt1–Pt2–P3 and P2–Pt1–Pt2–P4 of 23.8° (14.4°) and 19.7° (17.8°), respectively. A large twist was also noted in $Rh_2(\mu\text{-}S)(CO)_2(dppm)_2$.[1] No explanation for the twist was given, although close contacts of dppm phenyl rings with the terminal carbonyls were noted. Hoffman and Hoffmann concluded that there are no electronic reasons for the twist.[3] Steric factors are clearly involved in the structure of **3**. Nonbonded distances to the hydrogen atoms (calculated positions) are given in Table VI. Steric interactions between the phenyl rings and the terminal groups Cl1 and Cl2 are apparent. In addition, there are strong interactions of Cl3 and Cl4 of the $HgCl_2$ unit with the phenyl rings of the P2 and P3 portions of the dppm ligands. The result of these interactions is that the P1 and P4 portions of the dppm ligand are "pushed" toward the apex while the P2 and P3 portions are "pushed" away from the apex, giving the observed twist. This can also be seen when the angles Hg–Pt2–P3 (99.1° (97.8°)) and Hg–Pt1–P2 (95.5° (97.5°)) are compared with the angles Hg–Pt2–P4 (82.8° (86.2°)) and Hg–Pt1–P1 (82.9° (88.2°)).

The geometry about the Hg and Pt atoms is irregular. Pt and Pd usually assume square-planar geometries in "A-frame" complexes.[12,13] For the Pt in **3** to be square planar (neglecting the Pt–Pt bond), Cl1 and Cl2 should be trans to the Hg atom. Instead, angles for Hg–Pt1–Cl1 and Hg–Pt2–Cl2 are 142.4° (138.6°) and 140.0° (140.4°), respectively. A similar distortion was found for several Rh "A-frame" complexes.[14] Hoffman and Hoffmann analyzed this distortion in terms of a Walsh diagram, which indicated that in the more common undistorted complexes the bonding/antibonding interactions in the b_2 HOMO (the orbital formed from the apex group b_2 orbital) prevented distortion from the trans square-planar geometry. In the distorted complexes, which have two fewer electrons than the undistorted complexes, depopulation of the b_2 orbital allows "trends in the lower filled orbitals" to determine the geometry.[3] Since **3** is also distorted, the b_2 orbital must not be populated or it must have a significantly different character. This is to be expected if, as the NMR data discussed above suggest, the interaction of the $HgCl_2$ group is predominantly of a_1 symmetry.

Another indication of the absence of any b_2 interaction is the orientation of the $HgCl_2$ group. A b_2 interaction of an ML_2 fragment as considered by Hoffman and Hoffmann requires a planar geometry about M.[3] The observed geometry about the Hg atom in **3** is between planar and tetrahedral. The angle between the Hg coordination planes containing Pt1, Pt2, and Hg and Cl3, Cl4, and Hg is 57.2° (63.5°). This is less than the 90° angle expected for the tetrahedral geometry but is considerably larger than the 0° angle expected for a planar geometry. For a totally symmetric a_1 interaction the orientation would be determined by steric factors. Nonbonded distances to the hydrogen atoms (Table VI) show that the $HgCl_2$ orientation is determined by steric factors. The $HgCl_2$ chlorine atoms are "trapped" between the methylene group hydrogens and phenyl hydrogens with close contacts of the methylene hydrogens with Cl3 (2.75 Å (3.04 Å)) and Cl4 (2.93 Å (2.75 Å)) and phenyl ring hydrogen contacts of 2.89 Å (2.71 Å) between H46 and Cl3 and 2.74 Å (2.85 Å) between H86 and Cl4.

The Pt–Pt bond is retained upon coordination of the $HgCl_2$ group to $Pt_2Cl_2(dppm)_2$ with an increase from 2.652 (2)[15] to 2.7119 (8) Å in molecule A. In molecule B this distance is significantly larger at 2.7361 (9) Å, indicating a susceptibility of this bond length to packing forces. The P–Pt–P twist discussed above may be related to this distance since molecule B has a smaller twist than molecule A (see the torsional angles given above). The Pt–Pt bond distances in **3** are significantly shorter than that found in $[Pt_2Me_2(\mu\text{-}H)(dppm)_2]^+$ (2.932 (1) Å).[12] In the latter case the terminal methyl groups may contribute to an increased Pt–Pt bond length.

The Pt–Hg bond lengths of 2.7122 (8) and 2.7153 (7) Å (2.6991 (8) and 2.7097 (8) Å) are shorter than those observed in other Pt–Hg clusters (2.931–3.084 Å).[16] However, in these other clusters Hg is bridging from three to six Pt atoms. To our knowledge there are no examples of $HgCl_2$ bridging just two Pt atoms. In fact, we have found only one other example of $HgCl_2$ bridging two metal atoms, $Cp_2Rh_2(\mu\text{-}HgCl_2)(\mu\text{-}CO)(dppm)$, with an average Rh–Hg distance of 2.718 Å.[17] With use of the differences in Rh–P and Pt–P distances to calculate the difference in metal radii (0.034 Å), the equivalent M–Hg distance for the Rh complex (2.752 Å) is slightly longer than that in **3**.

The distances and angles in the dppm ligands are unexceptional. The Pt–P distances are in the range observed for other trans-dppm structures.[13,15] The Pt–Cl distances (2.330 (4)–2.350 (4) Å) are shorter than those observed in **2** (2.406 (6)–2.414 (6) Å)[15] and are slightly shorter than those observed in undistorted Pt and Pd "A-frame" complexes with terminal chlorides (2.360 (5)–2.435 (15) Å).[13] Short Rh–Cl distances were also observed in distorted $Rh_2(\mu\text{-}SO_2)Cl_2(dppm)_2$,[14] suggesting that these distances are related to the distortion about the metal. This is reasonable since the b_2 HOMO of the undistorted complexes is M–Cl antibonding[3] and this orbital is not occupied in the distorted complexes.

Conclusions

The original prediction by Hoffman and Hoffmann of stable "A-frame" clusters was based on the isolobal relationship of transition-metal ML_2 d^{10} and ML_4 d^8 fragments with the methylene group. While $HgCl_2$ is formally a ML_2 d^{10} fragment, the position of Hg as a post transition metal leads to significant differences between the bondings of $HgCl_2$ and CH_2 to the $Pt_2Cl_2(dppm)_2$ fragment. The low energy of the d orbitals of Hg limits their participation in the cluster bonding such that the b_2 interaction is absent, leaving only the a_1 interaction. In this regard $HgCl_2$ can be considered isolobal with H^+. Since $[AuL]^+$ and H^+ are also isolobal,[18] we can predict the existence of a trimetallic "A-frame" cluster with $X = [AuL]^+$ similar to the $HgCl_2$ cluster reported here. $[Pt_2(\mu\text{-}AuL)Cl_2(dppm)_2]^+$ should be readily accessible from $Pt_2Cl_2(dppm)_2$ and $[AuL]^+$. A series of trimetallic

---

(12) Brown, M. P.; Cooper, S. J.; Frew, A. A.; Manojlovic-Muir, Lj.; Muir, K. W.; Puddephatt, R. J.; Thompson, M. A. *J. Chem. Soc., Dalton Trans.* **1982**, 299–305; *J. Organomet. Chem.* **1980**, *198*, C33–C35.

(13) Brown, M. P.; Keith, A. N.; Manojlovic-Muir, Lj.; Muir, K. W.; Puddephatt, R. J.; Seddon, K. R. *Inorg. Chim. Acta* **1979**, *34*, L223–L224. Balch, A. L.; Lee, C.-L.; Lindsay, C. H.; Olmstead, M. M. *J. Organomet. Chem.* **1979**, *177*, C22–C26. Balch, A. L.; Benner, L. S.; Olmstead, M. M. *Inorg. Chem.* **1979**, *18*, 2996–3003.

(14) Cowie, M.; Dwight, S. K. *Inorg. Chem.* **1980**, *19*, 209–216, 2508–2513.

(15) Brown, M. P.; Puddephatt, R. J.; Rashidi, M.; Manojlovic-Muir, Lj.; Muir, K. W.; Solomun, T.; Seddon, K. R. *Inorg. Chim. Acta* **1977**, *23*, L33–L34. Manojlovic-Muir, Lj.; Muir, K. W.; Solomun, T. *Acta Crystallogr., Sect. B: Struct. Crystallogr. Cryst. Chem.* **1979**, *B35*, 1237–1239.

(16) Yamamoto, Y.; Yamazaki, H.; Sakurai, T. *J. Am. Chem. Soc.* **1982**, *104*, 2329–2330. Albinati, A.; Moor, A.; Pregosin, P. S.; Venanzi, L. M. *J. Am. Chem. Soc.* **1982**, *104*, 7672–7673.

(17) Faraone, F.; Lo Schiavo, S.; Bruno, G.; Bombieri, G. *J. Chem. Soc., Chem. Commun.* **1984**, 6–7.

(18) Evans, D. G.; Mingos, D. M. P. *J. Organomet. Chem.* **1982**, *232*, 171–191.

Table V. Selected Intramolecular Angles (deg)

atom			molecule		atom			molecule	
1	2	3	A	B	1	2	3	A	B
Pt1	Hg	Pt2	59.96 (2)	60.78 (2)	P1	Pt1	P2	174.4 (1)	174.3 (1)
Pt1	Hg	Cl3	134.41 (9)	137.8 (1)	Hg	Pt2	Pt1	59.96 (2)	59.42 (3)
Pt1	Hg	Cl4	113.7 (2)	106.9 (2)	Hg	Pt2	Cl2	140.0 (1)	140.43 (9)
Pt2	Hg	Cl3	102.04 (9)	114.9 (1)	Hg	Pt2	P3	99.13 (9)	97.77 (9)
Pt2	Hg	Cl4	139.8 (1)	132.4 (1)	Hg	Pt2	P4	82.77 (9)	86.2 (1)
Cl3	Hg	Cl4	106.0 (1)	103.7 (1)	Pt1	Pt2	Cl2	160.0 (1)	160.07 (9)
Hg	Pt1	Pt2	60.08 (2)	59.80 (3)	Pt1	Pt2	P3	87.09 (9)	89.80 (9)
Hg	Pt1	Cl1	142.4 (2)	138.6 (1)	Pt1	Pt2	P4	96.8 (2)	96.0 (1)
Hg	Pt1	P1	82.88 (9)	88.2 (2)	Cl2	Pt2	P3	87.8 (1)	85.7 (1)
Hg	Pt1	P2	95.47 (9)	97.53 (9)	Cl2	Pt2	P4	88.6 (1)	88.6 (1)
Pt2	Pt1	Cl1	157.5 (2)	161.5 (1)	P3	Pt2	P4	176.1 (1)	174.2 (1)
Pt2	Pt1	Pt1	95.59 (9)	95.2 (2)	Pt1	P1	P3	80.8 (1)	83.5 (1)
Pt2	Pt1	P2	88.3 (1)	88.2 (1)	Pt1	P2	P4	88.7 (1)	89.1 (1)
Cl1	Pt1	P1	91.0 (1)	88.7 (1)	Pt2	P3	P1	89.1 (1)	88.8 (1)
Cl1	Pt1	P2	87.0 (1)	86.6 (1)	Pt2	P4	P2	81.4 (1)	82.7 (1)

Table VI. Intramolecular Distances to Hydrogen Atoms (Å)

molecule A			molecule B		
atom			atom		
1	2	dist	1	2	dist
Pt1	H22	3.04	Pt1	H16	3.03
Pt1	H76	2.94	Pt1	H76	2.82
Pt2	H36	2.84	Pt2	H36	2.82
Pt2	H62	2.93	Pt2	H52	3.07
Cl1	H16	2.84	Pt2	H62	3.07
Cl1	H22	3.05	Cl1	H16	2.85
Cl1	H76	2.99	Cl1	H22	2.58
Cl2	H62	3.06	Cl2	H36	3.08
Cl3	H1	2.75	Cl2	H52	2.95
Cl3	H46	2.90	Cl2	H62	2.89
Cl4	H3	2.93	Cl3	H1	3.04
Cl4	H86	2.74	Cl3	H46	2.71
			Cl4	H3	2.75
			Cl4	H86	2.84

clusters based on this relationship was recently prepared from $Cp_2Rh_2(CO)(dppm)$.[19]

Experimental Section

General Procedures. All experiments were performed in air. Reagent grade solvents were stored over 3-Å molecular sieves under dinitrogen. $Pt_2Cl_2(dppm)_2$ was prepared by a published procedure.[8] Reagent grade $HgCl_2$ was used as received. NMR shifts are reported in ppm and referenced to Me_4Si for ^1H (90 MHz) and to external H_3PO_4 for ^{31}P (109 MHz). The ^{31}P NMR spectra were obtained in the decoupled mode. NMR spectra were run at ambient probe temperatures (28 ± 5 °C) except where noted.

Preparation of $Pt_2(\mu\text{-}HgCl_2)Cl_2(dppm)_2$ (3). Solid $HgCl_2$ (11 mg, 0.041 mmol) was added to a stirred solution of $Pt_2Cl_2(dppm)_2$ (50 mg, 0.041 mmol) in 4 mL of CH_2Cl_2. The $HgCl_2$ rapidly dissolved, and the solution turned from yellow to orange. Ether (10 mL) was added, and the solution was left to stand overnight. Large orange plates were recovered by decantation; 82% yield based on 0.5 CH_2Cl_2 of crystallization per formula unit. A small amount of $Pt_2Cl_2(dppm)_2$ was recovered from the supernatant.

Although these crystals readily lost CH_2Cl_2 on exposure to vacuum or to the atmosphere, complete removal required recrystallization from $CHCl_3$–Et_2O. These CH_2Cl_2-free crystals were used for the ^1H NMR studies. ^1H NMR ($CDCl_3$): 7.16–7.96 (m, Ph), 5.37 (m, $^2J_{HH}$ = 13.8 Hz, $^3J_{PtH}$ = 11.4 Hz, CH_2), 4.56 (m, $^2J_{HH}$ = 13.8 Hz, $^2J_{PH}$ = 2.0 Hz, $^3J_{PtH}$ = 97.8 Hz, CH_2). The spectrum in the P–CH_2–P region looks similar to that published for $Pt_2(\mu\text{-}CH_2)Cl_2(dppm)_2$.[20] For ^{31}P NMR spectra see Table I.

Structure Analysis. An outline of crystallographic and data collection parameters is given in Table II. A large plate grown from CH_2Cl_2–Et_2O as described above was cleaved, and a fragment was wedged and flame-sealed in a glass capillary filled with CH_2Cl_2 vapor. Cell dimensions were based upon a Delaunay reduction of a cell obtained from the centering of 25 reflections on the diffractometer.

Intensity data (294 K) were measured by the θ–2θ step scan technique with Mo Kα radiation from a graphite monochromator. The intensities of three standard reflections were measured after each 7200-s exposure to the X-rays and showed no intensity decay during the experiment. Averaging of equivalent reflections gave 8393 data points (agreement factor of 0.012 on F_o), of which 5698 had $F_o > 3\sigma(F_o)$ and 5773 had $F_o > 2\sigma(F_o)$ ($\sigma^2(F_o) = \sigma(\text{counting})^2 + (0.05F_o^2)^2$ and $\sigma(F_o) = \sigma(F_o^2)/2F_o$). Data with $F_o > 2\sigma(F_o)$ were used to refine the structure. The Enraf-Nonius SDP program package was used in all calculations.

The structure was resolved by direct and Fourier methods. Least-squares refinement minimizing $\sum w(|F_o| - |F_c|)^2$, where $w = 1/\sigma^2(F_o)$, converged with $R = \sum||F_o| - |F_c||/\sum|F_o| = 0.032$ and $R_w = [\sum(|F_o| - |F_c|)^2/\sum wF_o^2]^{1/2} = 0.041$. Hydrogen atoms were placed in "ideal" X-ray positions and were not refined. Two partially occupied positions for CH_2Cl_2 molecules were located. Refinement of each molecule at 0.5 occupancy gave reasonable thermal parameters. Within the two tetrahedrons the C–Cl bond distances ranged from 1.46 to 1.65 Å and the two bond angles were 130 and 137°. The final difference Fourier had the seven largest peaks (0.923–1.256 e/Å^3) in the vicinity of the two solvent molecules. No extinction correction was applied. The maximum parameter shift on the last cycle was less than 0.36 times its esd. The error in an observation of unit weight was 1.688. Atomic scattering factors were taken from ref 21. Final atomic positional parameters for the refined atoms are included in Table III. Selected intramolecular distances and angles are given in Tables IV and V.

Originally, the structure was refined with isotropic carbon and solvent chlorine atom thermal parameters to R = 0.035 and R_w = 0.046. However, the isotropic thermal parameters were exceptionally large (10–15 Å^2) for several of the ring carbons (not uncommon in dppm "A-frame" complexes). The rings that contained the carbon atoms with the high thermal parameters and the solvent chlorine atoms were then refined with anisotropic thermal parameters. Two of the carbons ended with non-positive-definite thermal parameters. Since this did not seem to significantly affect the overall structure, refinement was stopped at this point.

Acknowledgment. Support of this research by the Research Corp. is gratefully acknowledged. We thank the National Science Foundation for partial purchase of the X-ray (Grant No. CHE-7820347) and NMR (Grant No. PCM-8115599) equipment.

Registry No. **2**, 61250-65-5; **3**, 104531-57-9; Pt, 7440-06-4; Hg, 7439-97-6.

Supplementary Material Available: Tables of thermal parameters, calculated hydrogen atom positional parameters, remaining bond distances and angles, torsion angles, and weighted least-squares planes and an ORTEP drawing of molecule B (15 pages); a table of observed and calculated structure factors (16 pages). Ordering information is given on any current masthead page.

---

(19) Lo Schiavo, S.; Bruno, G.; Nicolo, F.; Piraino, P.; Faraone, F. *Organometallics* **1985**, *4*, 2091–2096. Bruno, G.; Lo Schiavo, S.; Piraino, P.; Faraone, F. *Organometallics* **1985**, *4*, 1098.

(20) Brown, M. P.; Fisher, J. R.; Puddephatt, R. J.; Seddon, K. R. *Inorg. Chem.* **1979**, *18*, 2808–2813.

(21) *International Tables for X-ray Crystallography*; Kynoch: Birmingham, England, 1974; Vol. IV.